THE JOURNAL OF BIOLOGICAL CHEMISTRY
Vol. 272, No. 23, Issue of June 6, pp. 14805–14809, 1997
Printed in U.S.A.

A Novel Tetrodotoxin-sensitive, Voltage-gated Sodium Channel Expressed in Rat and Human Dorsal Root Ganglia*

(Received for publication, January 29, 1997, and in revised form, April 2, 1997)

Lakshmi Sangameswaran‡, Linda M. Fish, Bruce D. Koch, Douglas K. Rabert, Stephen G. Delgado, Mariola Ilnicka, Lyn B. Jakeman§, Sanja Novakovic, Kimberley Wong, Ping Sze, Elda Tzoumaka, Gregory R. Stewart¶, Ronald C. Herman‖, Hardy Chan, Richard M. Eglen, and John C. Hunter

From the Center for Biological Research, Neurobiology Unit, Roche Bioscience, Palo Alto, California 94304

Dorsal root ganglion neurons express a wide repertoire of sodium channels with different properties. Here, we report the cloning from rat, dorsal root ganglia (DRG), cellular expression, and functional analysis of a novel tetrodotoxin-sensitive peripheral sodium channel (PN), PN1. PN1 mRNA is expressed in many different tissues. Within the rat DRG, both the mRNA and PN1-like immunoreactivity are present in small and large neurons. The abundance of sodium channel mRNAs in rat DRG is rBI > PN1 PN3 >>> rBIII by quantitative reverse transcription-polymerase chain reaction analysis. Data from reverse transcription-polymerase chain reaction and sequence analyses of human DRG and other human tissues suggest that rat PN1 is an ortholog of the human neuroendocrine channel. In *Xenopus* oocytes, PN1 exhibits kinetics that are similar to rBIIa sodium currents and is inhibited by tetrodotoxin with an IC_{50} of 4.3 ± 0.92 nM. Unlike rBIIa, the inactivation kinetics of PN1 are not accelerated by the coexpression of the β-subunits.

Voltage-gated sodium channels play a critical role in the rising phase of action potential and are, thus, important for impulse generation and conduction in most excitable cells. Sodium channels are integral membrane proteins that are usually comprised of one large α-subunit (>200 kDa) and one or more smaller β-subunits (1, 2). Several α-subunit sodium channel genes have been isolated from different tissues and functionally analyzed in heterologous expression systems (3). We and others have previously isolated clones from a dorsal root ganglia (DRG)[1] cDNA library for a novel tetrodotoxin-resistant sodium channel, PN3/SNS, which is expressed only in sensory neurons (4, 5). In addition to the PN3 cDNA clones, we have isolated cDNAs for other known and novel sodium channels (4). One of them, PN1 (peripheral sodium channel 1) (PN1), is a sodium channel that is regulated by nerve growth factor in PC12 cells (6, 7). Nerve growth factor increases the mRNA expression levels of brain type II/IIa and PN1 by two distinct signaling mechanisms (7). To further understand the molecular basis of neuronal excitability, we now describe the isolation of full-length cDNA clones for PN1, quantitation of PN1 mRNA levels as compared with other sodium channels in DRG, tissue distribution and its cellular localization in DRG, and functional characterization of this TTX-sensitive sodium channel in *Xenopus* oocytes. In addition, we discuss the isolation of partial clones of the human ortholog of PN1 (human neuroendocrine channel (hNE)) and the distribution of hPN1/NE sodium channel by RT-PCR analysis. Our studies indicate that PN1 is a novel TTX-sensitive sodium channel that is highly homologous to the rabbit sodium channel Nas (8) and expressed in a wide variety of tissues, including all cell types within the DRG, and that the human PN1 ortholog is, indeed, the neuroendocrine channel, hNE (9).

EXPERIMENTAL PROCEDURES

cDNA Cloning—Two rat DRG cDNA libraries, one oligo(dT) and the other random hexamer-primed, were constructed and screened as described (4). The cDNA probe for screening the random-primed cDNA library was a cDNA fragment from domains I and II of an rBIIa clone (10). Overlapping cDNA clones 27.6, 62.5, and 69.1 were assembled in the *Xenopus* oocyte expression vector, pBSTA (16), at the *Avr*II/*Bsp*EI sites. The overlapping cDNA clones 27.6, 62.5, 63.1, and 69.1, the resulting clones at various stages of assembly, and the final pBSTA-PN1 clone were sequenced on both strands. Sequence analyses were performed as described previously (4).

RT-PCR Analysis—Human tissues were provided by the Department of Pathology, Stanford University, Palo Alto, CA. Total RNA from human adrenal, heart, and brain tissues, and poly(A)$^+$ RNA from thyroid tissue were purchased from CLONTECH (Palo Alto, CA). Extraction of total RNA and synthesis of first strand cDNA from rat and human tissues were as described earlier (4). Tissue distribution analysis and quantitative RT-PCR (QRT-PCR) were performed with primer sets within the 3′-noncoding region of the gene. The forward primers targeted the same sequence, whereas the reverse primer for QRT-PCR was more upstream in the noncoding region. The amplicon sizes for tissue distribution analysis and the QRT-PCR experiment were 646 and 180 bp, respectively. Thermal cycler parameters were 30 s at 94 °C, 30 s at 61 °C, 1 min at 72 °C (34 cycles) and 30 s at 94 °C, 30 s at 61 °C, 5 min at 72 °C (1 cycle). For QRT-PCR, 100 ng total RNA were reverse transcribed to single-stranded cDNA, and the PCR was performed in the presence of 1 μCi [32P]dCTP and the following parameters: 30 s at 94 °C, 30 s at 55 °C and 2 min at 72 °C (35 cycles). Specific primers targeting the 3′-noncoding region for PN3, rBI, and rBIII were similarly employed for QRT-PCR. An aliquot of the reactions was run on a polyacrylamide gel that was dried prior to quantitation on a PhosphoImager (Bio-Rad). An external control cRNA comprising the same fragment was constructed for QRT-PCR as described by Ramakrishnan *et*

* The costs of publication of this article were defrayed in part by the payment of page charges. This article must therefore be hereby marked "*advertisement*" in accordance with 18 U.S.C. Section 1734 solely to indicate this fact.

‡ To whom correspondence should be addressed: Dept. of Molecular Pharmacology, Center for Biological Research, Neurobiology Unit, Roche Bioscience, 3401 Hillview Ave., Palo Alto, CA 94304. Tel.: 415-354-2098; Fax: 415-354-7363, E-mail: lakshmi.sangameswaran@roche.com.

§ Present address: Dept. of Physiology, 302 Hamilton Hall, Ohio State University, 1645 Neil Ave., Columbus, OH 43210.

¶ Present address: Alza Corp., 950 Page Mill Rd., Palo Alto, CA 10950.

‖ Present address: Calydon, 1014 Hamilton Ct., Menlo Park, CA 94025.

[1] The abbreviations used are: DRG, dorsal root ganglia; PN, peripheral sodium channel; TTX, tetrodotoxin; hNE, human neuroendocrine channel; RT, reverse transcription; PCR, polymerase chain reaction; QRT-PCR, quantitative RT-PCR; bp, base pair; PBS, phosphate-buffered saline; TEVC, two-electrode voltage clamp; kb, kilobase(s).

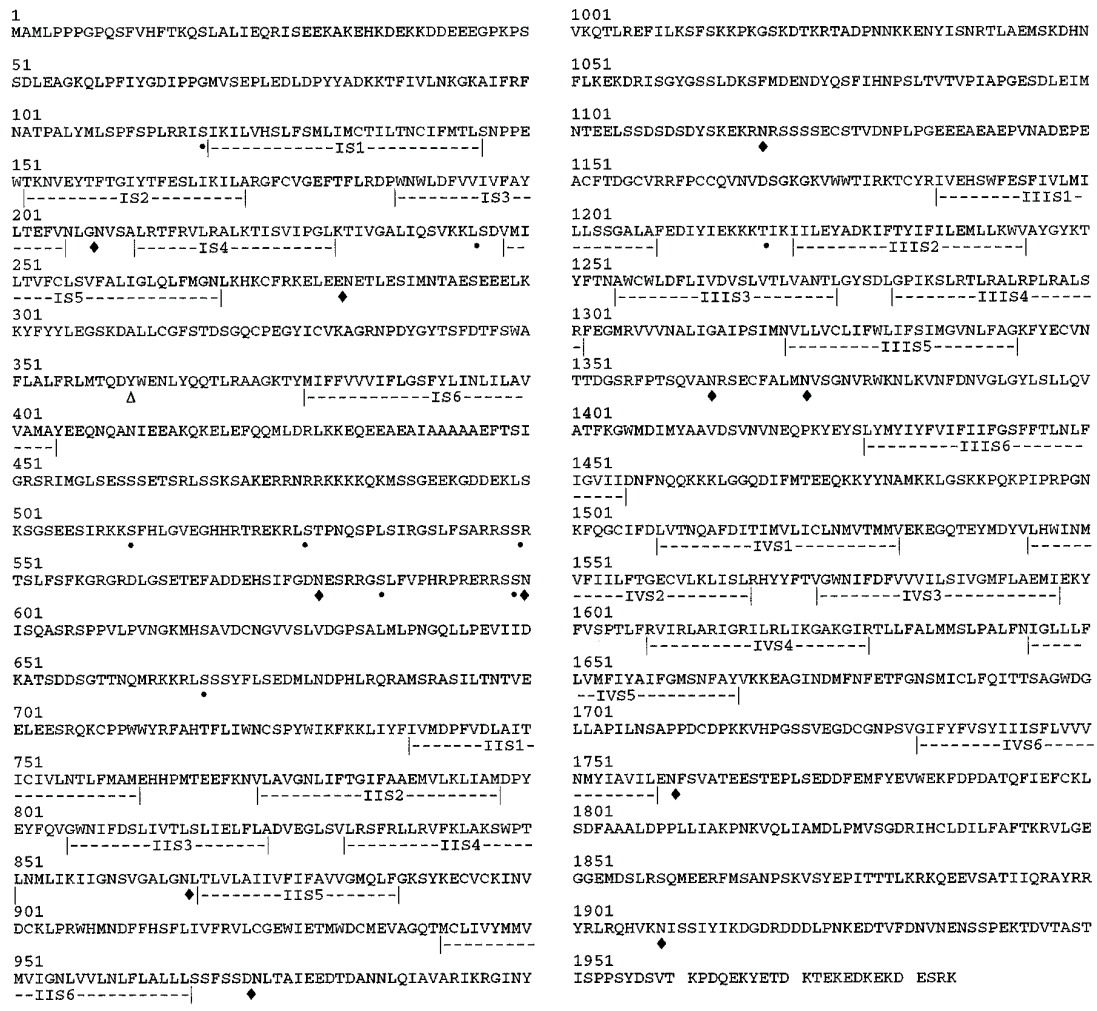

FIG. 1. **Primary structure of peripheral sodium channel 1 (PN1) deduced from the nucleotide sequence.** Putative transmembrane domains are *underlined*. ●, potential cAMP-dependent phosphorylation site; ♦, potential *N*-glycosylation site; △, TTX-sensitivity site.

al. (11). A standard curve was generated with the external controls for every experiment. 1 ng of pBK-PN1 plasmid DNA was included as positive control for the tissue distribution analysis by RT-PCR. Primers for glyceraldehyde-3-phosphate dehydrogenase were employed to demonstrate tissue viability (4) and to normalize the RNA content in QRT-PCR experiments.

Nested, degenerate primers from cloned human sodium channel sequences (12–15) were used to amplify a 687-bp fragment spanning domain IVS1 to IVS6. Thermal cycler parameters were: first set of primers, 1 min at 94 °C, 2 min at 50 °C, 4 min at 72 °C (34 cycles) and 1 min at 94 °C, 2 min at 50 °C, 8 min at 72 °C (1 cycle); and for the second set of primers, 1 min at 94 °C, 2 min at 55 °C, 4 min at 72 °C (34 cycles) and 1 min at 94 °C, 2 min at 55 °C, 8 min at 72 °C (1 cycle). Specific primers for interdomain I/II and interdomain II/III based hNE channel sequence (9) defined amplicon sizes of 813 and 352 bp, respectively. Thermal cycler parameters were: 30 s at 94 °C, 30 s at 60 °C, 2 min at 72 °C (35 cycles) and 30 s at 94 °C, 30 s at 60 °C, 7 min at 72 °C (1 cycle). Blots were prepared from the agarose gels that were used to fractionate the PCR fragments and hybridized with a ^{32}P-labeled DNA probe representing the entire coding sequence of the hNE channel (9).

In Situ Hybridization—Rats (125–150 g, Fisher and Charles River) were anesthetized with 10% chloral hydrate and perfused with phosphate-buffered saline (PBS) followed by 4% paraformaldehyde (pH 7.6). DRG (L4–5) were dissected out, cryoprotected by incubation in PBS-sucrose (10–20%), then frozen and sectioned (10 μm) with a cryostat. Sections were thawed, digested in proteinase K (1 μg/ml) for 1 h at 37 °C, dehydrated in ethanol (50–100%), and air dried. Specific activity of the oligonucleotide probes (targeted for the 3′-untranslated region of PN1 mRNA) was 5×10^7 cpm/μg. Hybridization, washing conditions, and development of sections were identical to those used for PN3 *in situ* hybridization (4). Selected sections were counterstained with propidium iodide. To perform *in situ* hybridization using non-radioactive oligonucleotide probes, the following protocol was used. After dewaxing/deparaffinization series in xylene and ethanol, 4-μm sections were permeabilized with Triton X-100 (0.3%, 15 min, RT) and subsequently with HCl (0.2 M), pepsin (0.1%, 10 min, 37 °C), and proteinase K (10 mg/ml, 30 min, 37 °C). Following the permeabilization, sections were postfixed in 4% formaldehyde, washed in PBS**,** and acetylated on a shaking platform with acetic anhydride (0.25%, in triethanolamine buffer, pH 8). Sections were pre-hybridized for 2 h at 37 °C in a hybridization solution containing 2 × SSC buffer, 1 × Denhardt's solution, 10% Dextran sulfate, 250 mg/ml yeast tRNA, 0.05 pM/ml of Randomer Oligoprobe (DuPont), 0.1 mg/ml poly(A) (Boehringer Mannheim), 500 mg/ml of denatured salmon testis DNA, and 50% deionized formamide. Hybridization was done in the same solution, containing specific antisense or sense oligoprobe, overnight at 37 °C. Following hybridization, samples were washed twice with 2, 1, and 0.25 × SSC, for 15 min at 37 °C each, followed by a rinse in buffer A (100 mM Tris-HCl (pH 7.5) plus 150 mM NaCl). Next, samples were incubated in blocking solution (buffer A plus 0.1% Triton X-100 plus 150 mM NaCl, 1 h, RT) and then in anti-digoxigenin antibodies conjugated with alkaline phospatase (2 h, RT). Samples were subsequently washed in buffer A, incubated in detection buffer (100 mM Tris-HCl plus 100 mM NaCl plus 50 mM $MgCl_2$), and then in 200 mM nitro blue tetrazolium/5-bromo-4-chloro-3-indolyl phosphate plus 10 mM of levamisol in 10 ml of detection buffer A (Boehringer Mannheim detection kit) overnight in the dark. Next day, sections were washed with water and mounted with Krystalon.

Antibody Preparation—Three peptides, two 16-mers and one 14-mer (located in interdomain I/II, II/III and domain IVS1/2), were synthesized according to the multiple antigen peptide technology. Polyclonal antisera were raised in rabbits (Research Genetics, AL) and affinity purified. The antipeptide antibody raised against the 16-amino acid peptide (1035–1050 amino acid in the protein sequence) located in the extracellular loop between domain IVS1 and S2 was employed in the

immunocytochemical localization of PN1 (see below).

Immunocytochemistry—Male Sprague-Dawley rats (200–250 g; Harlan, Indianapolis, IN) were anesthetized with 10% chloral hydrate and perfused with PBS followed by 10% formalin. Brain, DRG (L4–5), and lumbar spinal cord were removed and postfixed overnight in 10% formalin. Following fixation, tissue was embedded in paraffin and sectioned at 4 μm. After deparaffinization, sections were preincubated in PBS containing 20% normal goat serum and 0.2% Triton X-100 and incubated with PN1 antibodies (1/1000, overnight, at 4 °C). Tissue sections were washed, incubated in biotinylated anti-rabbit IgG (1/200, RT; Vectastain Elite) followed by peroxidase avidin-biotin complex (1/50, 90 min, RT; ABC, Vectastain Elite), and visualized with a diaminobenzidene reaction. Finally, the tissue sections were washed again, dehydrated, and coverslipped for light microscopy observations. For the control experiment, antibodies were preabsorbed with the corresponding peptide. A Nikon Microphot SA microscope was used for sample observation following both *in situ* hybridization and immunocytochemistry.

Oocyte Expression—cRNA was synthesized from PN1 subcloned into pBSTA (16) using an Ambion mMessage mMachine kit. Defolliculated *Xenopus* oocytes (stage V and VI) were prepared (17) and injected with PN1 cRNA using a Nanojector (Drummond). For two-electrode voltage clamp (TEVC) recordings, oocytes that had been injected with 30–60 pg of cRNA for 1–2 days previously were perfused with a solution containing (in mM) 81 NaCl, 2 KCl, 1 $MgCl_2$, 0.3 $CaCl_2$, and 20 HEPES-NaOH (pH 7.5), impaled with agarose-cushion electodes (0.3–0.8 megohm) (18), and voltage clamped with a GeneClamp 500 amplifier (Axon Instruments) in TEVC mode. Oocytes were held at −100 mV and pulsed to different voltages for 15 ms. For macropatch recordings, oocytes that had been injected with 10 ng of PN1 cRNA several days previously were devitellinized (20) after osmotic shrinkage in ND-96 (17, see below) plus 100 mM NaCl. The bath solution contained (in mM) 9.6 NaCl, 88 KCl, 1 $CaCl_2$, 1 $MgCl_2$, 11 EGTA, and 5 HEPES-KOH (pH 7.5). The bath electrode was electrically coupled to the bath via an agarose bridge (1% agarose in bath solution). 1.2–2.6 megohm patch elecrodes were pulled from either borosilicate (Garner Glass) or aluminosilicate (Sutter Instruments) glass on a horizontal puller (Sutter P-87) and filled with ND-96 (17), which contains (in mM) 96 NaCl, 2 KCl, 1.8 $CaCl_2$, 1 $MgCl_2$, and 5 Hepes-NaOH (pH 7.5). Borosilicate electrodes were coated with dental wax and firepolished before use. Recordings were made from attached macropatches using a GeneClamp (Axon Instruments) in patch clamp mode (CV5–1GU headstage). To the extent possible, pipette capacitance was compensated using the amplifier capacitance compensation. Voltages were not corrected for the liquid junction potential. Macropatches were held at −110 mV and were pulsed to different voltages for 9 ms. For both TEVC and macropatch recordings, stimulation and recording were controlled by a computer running pClamp 6.0.3 (Axon Instruments). Data was sampled at 50 kHz after filtering at 5 kHz (TEVC) or 10 kHz (macropatch) with a 4-pole Bessel filter. For activation data, P/−4 (TEVC) or P/−6 (macropatch) leak subtraction (19) was used. For macropatch recording, each pulse was repeated 5 times with digital on-line averaging. Steady-state inactivation curves used test pulses to +10 mV and were leak subtracted by calculating the passive leak, which was determined from the holding current at −100 mV and −120 mV after each test pulse.

TABLE I
Tissue distribution of rat PN1 and human NE/PN1 channel mRNAs by RT-PCR analysis

Tissue	rPN1	hNE/PN1
DRG	+	+
Nodose ganglia	+	ND[a]
SCG	+	ND
Sciatic nerve	+	+
Heart	+	+
Skeletal muscle	−	−
Thyroid	ND	+
Adrenal	ND	+
Brain	+	+
Spinal cord	ND	+

[a] ND, not determined.

RESULTS AND DISCUSSION

Primary Structure of PN1—The sequence of a clone from the RT-PCR analysis of rat DRG using degenerate primers, corresponding to rat sodium channel domain IV, indicated a novel voltage-gated sodium channel. Subsequently, this was found to be identical to part of the sequence of clone 27.6, isolated from the oligo(dT)-primed cDNA library. Nucleotide sequence analysis of the full-length cDNA assembled from clones 27.6, 62.5, and 69.1 revealed a 5952-base pair open reading frame coding for a 1984-amino acid protein (Fig. 1). In addition, clone 27.6 had a 3.3-kb 3′-noncoding sequence, and clone 63.1 had a

TABLE II
Quantitation of sodium channel mRNAs in rat DRG by QRT-PCR analysis

Sodium channel subtype	Total RNA ± S.D.
	pg/μg
PN1	5.69 ± 2.65
PN3	4.47 ± 2.65
rBI	17.18 ± 9.09
rBIII	0.0018 ± 0.0011

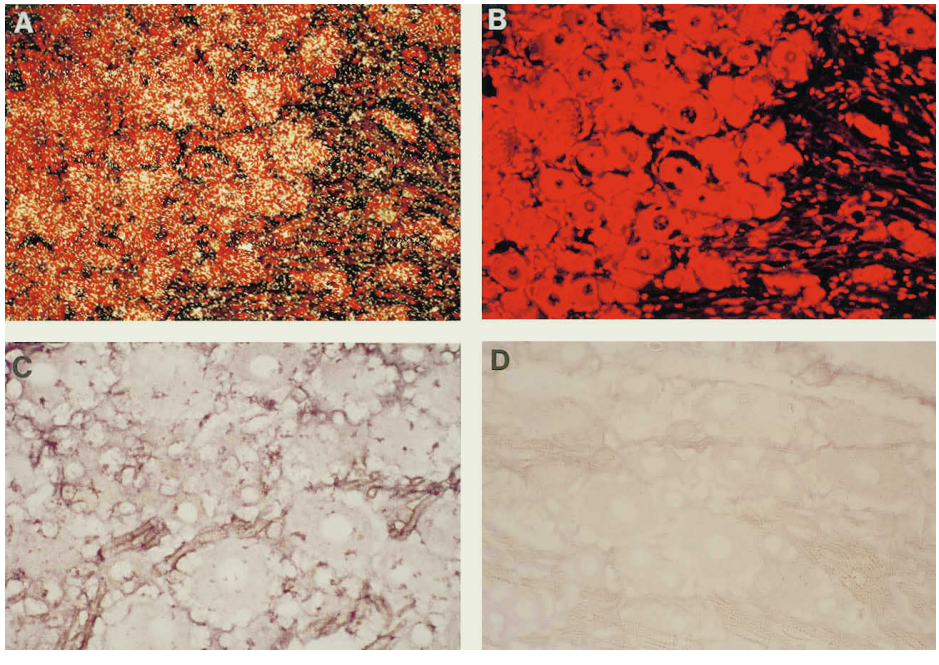

FIG. 2. **Distribution of PN1 mRNA in rat DRG neurons.** *A*, radioactive *in situ* hybridization of a 10-μm cryosection illustrating widespread distribution of PN1 mRNA in DRG neurons. *B*, propidium iodide counterstain of the same section showing localization and size of neurons (× 20). *C*, nonradioactive *in situ* hybridization of a 4-μm paraffin section. *D*, control with sense probe (× 40).

320-base pair 5′-noncoding upstream sequence. The assembled clone thus comprised 9.5 kb of the 11-kb band detected in Northern blots (see below; 6, 7). There was an out-of-frame ATG upstream of the genuine ATG, akin to other cloned sodium channels (10). All the hallmark features of the voltage-gated sodium channels were preserved in the deduced amino acid sequence of PN1, including consensus motifs for protein kinase A. Between segments 5 and 6 in domain I, there is the aromatic amino acid, Tyr, that confers sensitivity to low concentrations of TTX (see below) (20). PN1 shares highest homology with the human NE channel and rabbit NAS sodium channel (93% identity), rBII (79%), rBIII (78%), and rBI (78%). Indeed, PN1 mapped very close to the brain sodium channels, rBI, rBII, and rBIII in mouse chromosome 2 (21). A survey of the sodium channel α-subunits in the human DRG was performed by RT-PCR with nested, degenerate primers from domain IV. The nucleotide sequence of one of the clones from this region was identical to the hNE channel (data not shown; 8).

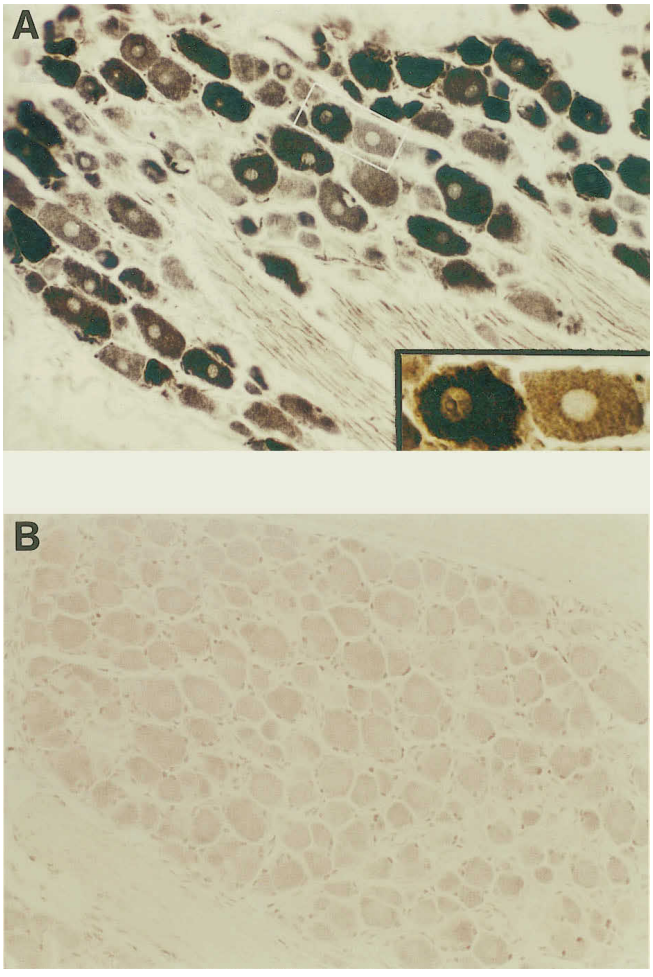

FIG. 3. **PN1 immunocytochemistry of DRG neurons.** *A*, immunolabeling with purified PN1 antibody showing that all neurons labeled with varying intensity (4-μm paraffin section, × 20). *Inset* (× 40) illustrates two neurons that are of similar size but labeled with different intensity. *B*, antibody control. DRG section was incubated with the PN1 antibody that had been preabsorbed with the peptide antigen (× 20).

Expression of PN1—Northern analyses with a cDNA probe from rBII revealed an 11-kB band that was intense in DRG and to a lesser extent in brain (data not shown; 6, 7). RT-PCR analyses (Table I) indicated that PN1 mRNA was expressed in a wide variety of rat tissues, except skeletal muscle. The mRNA levels of PN1, PN3, rBI, and rBIII in the adult rat DRG by QRT-PCR are presented in Table II, showing that PN1 and PN3 mRNAs were expressed at comparable levels. rBI mRNA was found to be more abundant than PN1 and PN3, and rBIII was the least abundant of all.

RNAs from a variety of human tissues were used to perform RT-PCR (Table I) with specific primers for hNE interdomains I/II and II/III, and the PCR products were characterized by sequence analysis and Southern blot hybridization under high stringency conditions. The results in Table I show that the hNE channel mRNA was expressed in the same tissues as rat PN1, including adrenal and thyroid tissues as was described by Klugbauer *et al.* (9). Neither hNE nor rat PN1 was expressed in skeletal muscle. The sequences of the PCR fragments spanning interdomains I/II and II/III amplified from DRG were identical to the hNE channel. Thus, cloning/detection of sequences spanning many regions of the coding sequence of hNE in human DRG demonstrated that the NE channel was expressed in this tissue. However, the disparity in mRNA sizes of rat PN1 (11 kB) and hNE/PN1 (9.5 kB) (9) will have to be resolved. It is likely that rat PN1 has a much longer 3′-untranslated region (3.3 kb) than hNE. The high sequence homology shared between rat PN1 and hNE, together with the above observation, suggests that hNE is the human ortholog of the rat PN1 and rabbit NAS sodium channels (8).

PN1 mRNA is expressed in small and large DRG neurons, as shown by radioactive *in situ* hybridization in Fig. 2*A*. Fig. 2*B* illustrates the same section labeled with propidium iodide to

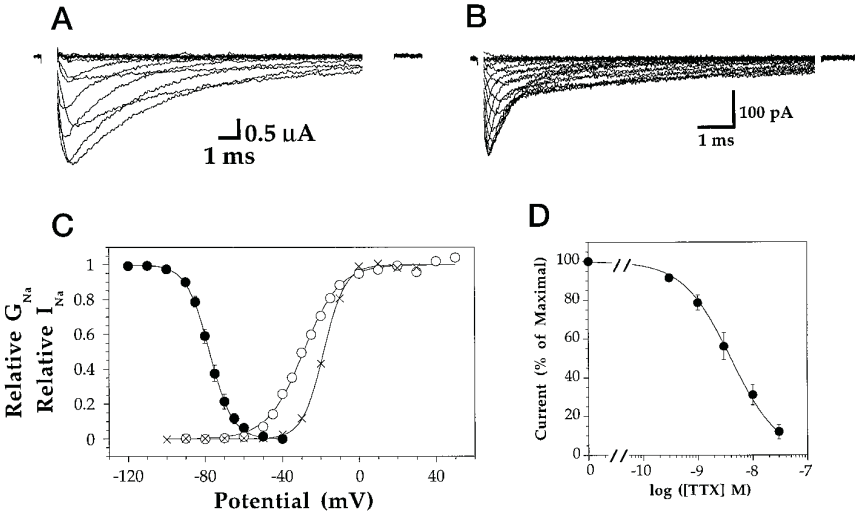

FIG. 4. **Inward currents induced in *Xenopus* oocytes by injection of PN1 cRNA.** *A*, shown is a two-electrode voltage clamp recording from a *Xenopus* oocyte that had been injected with 60 pg of PN1 cRNA two days earlier (holding potential = ×100 mV); *B*, recording from a cell-attached macropatch (holding potential = ×110 mV); *C*, graph of steady-state inactivation (10 s prepulses) curve using two-electrode voltage clamp (●) and conductance curves calculated from *A* (×) and *B* (○); and *D*, concentration-effect curve for TTX block of PN1 sodium current. To test channel blockade by TTX, oocytes were repeatedly depolarized from −100 mV to 0 mV for 5 ms at 0.033 Hz; P/-4 leak subtraction was used (19). These oocytes were superfused with solutions containing the indicated concentrations of TTX, and the peak current amplitudes were allowed to attain steady-state before the next, higher concentration of TTX was applied.

show the general morphological characteristics and size of neurons. Similar results were obtained with nonradioactive *in situ* hybridization (Fig. 2*C*). In agreement with the *in situ* hybridization data, immunocytochemistry with PN1 antipeptide antibody demonstrated that all DRG neurons labeled with varying intensity, but no particular pattern could be detected (Fig. 3*A*). In control experiments where the antibody preabsorbed with the peptide was used, there was hardly any immunoreactivity (Fig. 3*B*), thereby demonstrating the specificity of the antibody. In addition, a widespread distribution of PN1 immunoreactivity was observed in rat spinal cord and brain (data not shown).

Functional Analysis of PN1—TEVC recordings from *Xenopus* oocytes injected with PN1 cRNA (Fig. 4*A*) indicated that expression of PN1 produced an inward current that inactivated somewhat slowly compared with TTX-sensitive sodium currents found in brain, skeletal muscle, and DRG (22–24). The $V_{1/2}$ for activation using TEVC was -20 ± 2.0 mV, $k = -6.5 \pm 0.61$ mV ($n = 5$). Coexpression of the rat β1-subunit is known to accelerate the inactivation kinetics of the rBIIA, rBIII, and rat skeletal muscle (rSkM1) sodium channels recorded using TEVC, perhaps by stabilizing a fast gating mode (data not shown; 25, 26). Surprisingly, coinjection of PN1 cRNA with 5 ng of rβ1 (25) cRNA, 1 ng of rβ2 (27) cRNA, or a combination of rβ1 and rβ2 cRNAs did not appear to accelerate the inactivation kinetics (data not shown).

Due to the large capacitance of *Xenopus* ooctyes, the time resolution of TEVC is limited. To study PN1 currents with more temporal fidelity, we recorded from cell-attached macropatches of oocytes expressing high levels of PN1 (Fig. 4B). In these recordings, the $V_{1/2}$ for activation (Fig. 4*C*) was found to be -31 ± 3.8 mV, $k = -8.9 \pm 0.47$ mV ($n = 4$). This is similar to the voltage dependence of activation of rBIIA (28) and hH1 (29) using this recording technique. As expected, with the increased temporal resolution, the currents activated and inactivated much more rapidly (Fig. 4*B*). The inactivation was biphasic, with 55–60% of the current inactivating very rapidly while the rest inactivated with somewhat slower kinetics. Both phases of inactivation were voltage-dependent, with half times of 0.46 and 20 ms at -30 mV and 0.1 and 1.8 ms at $+10$ mV. These results are consistent with the idea that this channel exhibits more than one gating mode, as has been found for other sodium channels (26, 28–31).

Analysis of steady-state inactivation using TEVC and 10 s prepulses (Fig. 4*C*) yielded a $V_{1/2}$ of -78 ± 1.1 mV, $k = 5.8 \pm 0.41$ mV ($n = 4$). This voltage dependence is very close to that of hH1 using this protocol ($V_{1/2} = -78 \pm 1.6$ mV, $n = 11$) but more negative than that of rBIIA ($V_{1/2} = -65 \pm 1.2$ mV, $n = 15$).

The PN1 current was blocked by TTX with an IC_{50} of 4.3 ± 0.92 nM ($n = 4$; Fig. 3*D*). This indicates that PN1 is a TTX-sensitive sodium channel, with TTX sensitivity similar to that of the rBIIA (32), rSkM1 (33), rBIII (34, 35), and hNE (8) channels but with much higher sensitivity than the cardiac (36, 37) and PN3/SNS (4, 5) sodium channels.

In summary, PN1 is a novel voltage-gated sodium channel that is similar, but not identical, to previously characterized sodium channels, such as rBIIa. It is sensitive to low concentrations of TTX. However, in contrast to rBIIa, when recorded using TEVC, PN1 exhibits inactivation kinetics that are not accelerated by coexpression of the β-subunits. In DRG, PN1 appears to be expressed at significant levels that are comparable to those of PN3. Unlike PN3, PN1 is expressed in all types of neurons in DRG. In view of their high sequence homology, we believe that rat PN1, hNE, and rabbit NAS are orthologs of the same sodium channel gene. The wide distribution of PN1/hNE suggests that they contribute to excitability in several types of neurons and excitable cells.

Acknowledgments—We thank C. Yee, P. Zuppan, and C. Bach for sequence analysis and oligonucleotide synthesis and E. Shelton for input on PN1 antisera. We are grateful to A. Tischler for oocyte preparations and recording from rBIIa and hH1. We are also thankful to R. L. Whiting for keen interest and encouragement during the course of this work.

Note Added in Proof—While this publication was in review, the authors became aware of a paper (Toledo-Aral, J. T., Moss, B. L., He, Z., Koszowski, A. G., Whisenand, T., Levinson, S. R., Wolf, J. J., Siols-Santiago, I., Halegoua, S., and Mandel, G. (1997) *Proc. Natl. Acad. Sci. U. S. A.* **94,** 1527–1532) that describes the cloning of an identical gene, PN1 from PC12 cells and its expression in peripheral neurons.

REFERENCES

1. Catterall, W. A. (1992) *Physiol. Rev.* **72,** S15–S48
2. Isom, L. L., De Jongh, K. S., and Catterall, W. C. (1994) *Neuron* **12,** 1183–1194
3. Catterall, W. A. (1991) *Curr. Opin. Neurobiol.* **1,** 5–13
4. Sangameswaran, L., Delgado, S. G., Fish, L. M., Koch, B. D., Jakeman, L. B., Stewart, G. R., Sze, P., Hunter, J. C., Eglen, R. M., and Herman, R. C. (1996) *J. Biol. Chem.* **271,** 5953–5956
5. Akopian, A. N., Sivilotti, L., and Wood, J. (1996) *Nature* **379,** 257–262
6. D'Arcangelo, G., Paradiso, K., Sheperd, D., Brehm, P., Halegoua, S., and Mandel, G. (1993) *J. Cell. Biol.* **122,** 915–921
7. Toledo-Aral, J. J., Brehm, P., Halegoua, S., and Mandel, G. (1995) *Neuron* **14,** 607–611
8. Belcher, S. M., Zerillo, C. A., Levinson, R., Ritchie, J. M., and Howe, J. R. (1995) *Proc. Natl. Acad. Sci. U. S. A.* **92,** 11034–11038
9. Klugbauer, N., Lacinova, L., Flockerzi, V., and Hoffmann, F. (1995) *EMBO J.* **14,** 1084–1090
10. Auld, V. J., Goldin, A. L., Krafte, D. S., Marshall, J., Dunn, J. M., Catterall, W. A., Lester, H. A., Davidson, N., and Dunn, R. J. (1988) *Neuron* **1,** 449–461
11. Ramakrishnan, R., Fink, D. J., Jiang, G., Desai, P., Glorioso, J. C., and Levine, M. (1994) *J. Virol.* **68,** 1864–1873
12. Ahmed, C. M. I., Ware, D. H., Lee, S. C., Patten, C. D., Ferrer-Montiel, A. V., Schinder A. F., McPherson, J. D., Wagner-McPherson, C. B., Wasmuth, J. J., Evans, G. A., and Montal, M. (1992) *Proc. Natl. Acad. Sci. U. S. A.* **89,** 8220–8224
13. Gellens, M. E., George, A. L., Chen, L., Chahine, M., Horn, R., Barchi, R., and Kallen, R. G. (1992) *Proc. Natl. Acad. Sci. U. S. A.* **89,** 554–558
14. George, A. L., Komisarof, J., Kallen, R. G., and Barchi, R. L. (1992) *Ann. Neurol.* **31,** 131–137
15. George, A. L., Knittle, T. J., and Tamkun, M. M. (1992) *Proc. Natl. Acad. Sci. U. S. A.* **89,** 4893–4897
16. Goldin, A. L., and Sumikawa, K. (1992) *Methods Enzymol.* **207,** 279–297
17. Goldin, A. L. (1992) *Methods Enzymol.* **207,** 266–279
18. Schreibmayer, W., Lester, H. A., and Dascal, N. (1994) *Pfluegers Arch. Eur. J. Physiol.* **426,** 453–458
19. Benzanilla, F., and Armstrong, C. M. (1977) *J. Gen. Physiol.* **70,** 549–566
20. Kallen, R. G., Cohen, S. A., and Barchi, R. L. (1993) *Mol. Neurobiol.* **7,** 383–428
21. Kozak. C., and Sangameswaran, L. (1996) *Mamm. Genome* **7,** 787–788
22. Huguenard, J. R., Hamill, O. P., and Prince, D. A. (1988) *J. Neurophysiol.* **59,** 778–795
23. Franke, C., and Hatt, H. (1990) *Pfluegers Arch. Eur. J. Physiol.* **415,** 399–406
24. Elliott, A. A., and Elliott, J. R. (1993) *J. Physiol.* **463,** 39–56
25. Isom, L. L., De Jongh, K. S., Patton, D. E., Reber, B. F. X., Offord, J., Charbonneau, H., Walsh, K., Goldin, A. L., and Catterall, W. A. (1992) *Science* **256,** 839–842
26. Patton, D. E., Isom, L. L., Catterall, W. A., and Goldin, A. L. (1994) *J. Biol. Chem.* **269,** 17649–17655
27. Isom, L. L., Ragsdale, D. S., De Jongh, K. S., Westenbroek, R. E., Reber, B. F. X., Scheuer, T., and Catterall, W. A. (1995) *Cell* **83,** 433–442
28. Fleig, A., Ruben, P. C., and Rayner, M. D. (1994) *Pfluegers Arch. Eur. J. Physiol.* **427,** 399–405
29. Zhou, J., Potts, J. F., Trimmer, J. S., Agnew, W. S., and Sigworth, F. J. (1991) *Neuron* **7,** 775–785
30. Nilius, B. (1988) *Biophys. J.* **53,** 857–862
31. Moorman, J. R., Kirsch, G. E., VanDongen, A. M. J., Joho, R. H., and Brown, A. M. (1990) *Neuron* **4,** 243–252
32. Patton, D. E., and Goldin, A. L. (1991) *Neuron* **7,** 637–647
33. Gellens, M. E., George, A. L., Jr., Chen, L., Chahine, M., Horn, R., Barchi, R. L., and Kallen, R. G. (1992) *Proc. Natl. Acad. Sci. U. S. A.* **89,** 554–558
34. Trimmer, J. S., Cooperman, S. S., Tomiko, S. A., Zhou, J., Crean, S. M., Boyle, M. B., Kallen, R. G., Sheng, Z., Barchi, R. L., Sigworth, F. J., Goodman, R. H., Agnew, W. S., and Mandel, G. (1989) *Neuron 3,* 233–249
35. Suzuki, H., Beckh, S., Kubo, H., Yahagi, N., Ishida, H., Kayano, T., Noda, M., and Numa, S. (1988) *FEBS Lett.* **228,** 195–200
36. Joho, R. H., Moorman, J. R., VanDongen, A. M. J., Kirsch, G. E., Silberberg, H., Schuster, G., and Brown, A. M. (1990) *Mol. Brain Res.* **7,** 105–113
37. Cribbs, L. L., Satin, J., Fozzard, H. A., and Rogart, R. B. (1990) *FEBS Lett.* **275,** 195–200